Journal of Electrical and Computer Engineering Innovations
(JECEI)
Journal homepage: http://www.jecei.sru.ac.ir

Research paper

The Effects of the Model Predictive Controller Compared to the LQR Controller on the Optimal Distribution of the Suitable Load and the Creation of Balance in Microgrids

I. Sayedi[1], M.H. Fatehi[2], M. Simab[3]

[1]*Department of Electrical Engineering, Marvdasht Branch, Islamic Azad University, Marvdasht, Iran.*

[2]*Department of Electrical Engineering, Kazerun Branch, Islamic Azad University, Kazerun, Iran.*

[3]*Department of Electrical Engineering, Marvdasht Branch, Islamic Azad University, Marvdasht, Iran.*

Article Info

Article History:
Received 29 June 2021
Reviewed 01 August 2021
Revised 19 October 2021
Accepted 19 October 2021

Keywords:
DE-MPC
AC microgrid
Power sharing
Renewable energy sources
Finite control states
LQR controller

*Corresponding Author's Email Address:
Mh_fatehi@kau.ac.ir

Abstract

Background and Objectives: Distributed generation (DG) sources are modeled using an ideal DC voltage source connected to the microgrid via voltage source converters (VSCs). Model predictive control presents a distinct method for energy processing.

Methods: In this method, the electric power converter is considered a power amplifier with a discrete and nonlinear structure. Therefore, unlike linear control methods, the discrete and nonlinear nature of the converter is considered in this method. In this paper, the distributed model predictive controller was selected from among different methods of load allocation among DG sources due to its more advantages compared to the linear quadratic regulator (LQR) controller.

Results: It has been Proposed that we could obtain better results in predictive control, utilizing similarity transform in the state matrix and its modification. In this research, all the simulations have been performed in the MATLABSimpower environment of MATLAB software.

Conclusion: Moreover, to demonstrate the superior performance of the model predictive controller compared to the LQR controller, both performance modes of the microgrid, namely the grid-connected and islanding modes, have been considered.

Introduction

A microgrid is a power grid on a small scale that has been designed to supply electricity to end-users. Microgrids are capable of injecting their excess energy into the main grid under special circumstances. One of the most important challenges faced by the microgrid operator is maintaining the security and stability of the system [1]. Most renewable energy-based distributed generation (DG) sources require voltage source inverters (VSIs) to connect to the microgrid [2]. Nowadays, the control of industrial processes and the adoption of suitable methods for this purpose are of great importance. Industrial control methods must possess certain characteristics, including the following: Ease of use by the operator, simple adjustment, and economy [3].

Although the use of PID and linear quadratic regulator (LQR) controllers is common in the industry, it must be noted that industrial processes include a wide range of different behaviors, which limits the use of such controllers [4]. This wide range of dynamic behaviors is due to different factors, such as zeros outside the stable

region, unstable poles, and long delays that vary with time and are unknown. In voltage stability analysis, the presence of a numerical value or an index that indicates the stability status of the system is necessary and useful. The voltage range of the buses in the system cannot represent the stability status of the system's voltage in many cases. In a given system, all the voltages may be within the permissible range; however, a small disturbance may lead to voltage attenuation in the power system.

The model predictive control (MPC) method is a nonlinear control technique, in which the mathematical model of the system is used and the system's behavior is analyzed with respect to different inputs. This controller exhibits a considerably better behavior than the LQR controller in dynamic models and can provide better reliability than classical methods considering the nonlinear behavior [4].

Knowing the response of the system to a given input, one can determine the input in such a way that the reference value becomes equal to the actual value. Nevertheless, obtaining the best input signal to obtain the desired system response requires solving optimization problems, which involve tedious computations. Nonetheless, fortunately, the number of available cases for the input in switching power electronic systems is limited to cases where the switches are allowed to activate.

In this case, the computations are reduced. For example, in a three-phase four-wire system, a total of 24=16 switching states can be imagined. The model predictive control system checks all the 16 vectors, and the vector that produces the lowest control error is selected in the end [5]. The MPC algorithm is a method to deal with such complex processes. Implementing the model predictive control model for electric power converters can encounter problems due to the need for a large amount of computation for the real-time solution of optimization equations [6].

To resolve this problem, practical methods, such as the out-of-line calculation of the optimization equations and the solution of these equations using finite set switching, have been considered. The latter is known as the finite set model predictive control (FS-MPC) because this method operates using a number of finite and possible switching states of the electric power converter [7].

The FS-MPC method has so far been used in different applications as rectifier, motor control, and uninterruptible power supply (UPS). When FS-MPC designs are implemented experimentally, a large volume of computations is performed in the sampling period, which causes a considerable delay in the actuator signal [7].

Therefore, ignoring the delay due to measurement, computations, and actuator signal in the controller design will lead to the weak performance of the controller. In [8], the reason for this delay and the method of compensating it have been explained, in which an interruption occurs between when the current is measured and when the new switching state is applied. During this interruption, the previous switching state is present at the converter output, causing a difference between the load current and the reference current and increasing the current ripple. In [9] predicting the next two samples instead of the next sample has been used to address this issue. In [10], a novel MPC method, called the fast model predictive control, is presented.

This method has significantly reduced computations and can be used in multi-level converters with large numbers of control vectors. Another disadvantage of the FS-MPC method is the variable switching frequency. A variable switching frequency causes a wide range of harmonics at the converter output, which can lead to resonance and make filter design difficult. In [11], one can maintain the switching frequency constant by adding corrective terms to the cost function. Moreover, in [11], the current model MPC design has been modified in such a way that the switching frequency can be made almost independent of the sampling frequency.

Adjusting and selecting the weighting factors in the FS-MPC method is a considerable challenge and significantly affects the system performance. Adjusting these factors is more difficult and time-consuming than adjusting the PI controller parameters in classical current control and adjusting the hysteresis bandwidth. Ref. [12] has mentioned important guidelines for determining the optimal value of the weighting factors. In [13], an MPC method without the use of weighting factors has been introduced for induction motor drive applications. In this paper, by presenting a state feedback method and via optimal design using the iteration method, all the possible switching states along the predictor horizon have been defined for the controller. As such, the shortcomings of previous methods have been overcome [14].

In, the authors present an adaptive optimization method for NMPC, where a Kalman extended filter (KEF) is used for estimating the state variables. In [15], a system is investigated where the superheated steam temperature (SST) is the main variable that must be controlled. To do so, several categories of cascading PIDs have been used to control this variable. In [3], to adapt the model, neural networks are presented for controlling the model predictive control. In [16], a fuzzy method based on Lyapunov fragment functions is used in the model predictive control.

In [17], in order to make the system smart, generalized predictive control (GPC) and a neural network model are used.

In this method, a nonlinear neural network is used to extract the linear model of the system. In [18], horizon optimization is utilized for predictive control using a genetic algorithm.

In [19], the prediction of the next two samples is used instead of predicting the next sample. Moreover, [20] proposes a new predictive control method, called the fast predictive control.

In this method, the volume of calculations will be significantly reduced, and it can be used in multi-level converters that have a large number of control vectors. In addition, [21] modifies the current predictive control scheme in such a way that the switching frequency can become somewhat independent from the sampling frequency.

Increasing the sampling frequency improves the performance of FS-MPC, while reducing the ripple of the output current. However, increasing the sampling frequency also increases the switching frequency, which ultimately leads to increased losses [22], [23]. The current paper presents a predictive control method using the state feedback controller to control the switching interface converters and compensate for the unbalanced and nonlinear loads.

Furthermore, in addition to introducing several different structures for microgrids, including DG sources voltage source converters (VSCs), we will examine the impact of the proposed controllers, especially Distributed Economic Model Predictive Controller (DEMPC), on the performance of these microgrids. For this purpose, it has been proposed that we could obtain better results in predictive control, utilizing similarity transform in the state matrix and its modification. With this method, in addition to the fact that we have maintained system dynamics, we can use this similarity transform to evaluate all systems.

Hence, the following state transform matrix is considered for this system, and better results in terms of overshoot, rise time, settling time, and steady-state have been obtained with this method, which are shown in results paper. We will consider various conditions for microgrid loading. Unbalanced and nonlinear loads, which disrupt the balance of the grid and reduce the power quality, must be compensated for by the proposed controller comparison to FS_MPS and DVSM-MPC methods.

Study of a Microgrid Containing a DG Source

As mentioned in Fig.1, the system considered in this section contains a DG source. The microgrid is connected to the main grid at the point PCC. The DG source has local loads, including unbalanced and nonlinear loads.

In the grid-connected mode, the common load is fully supplied by the grid, and the power required for the local load is jointly supplied by the source DG-1 and the grid. In the islanding mode, i.e., when CB-1 is opened and the microgrid is disconnected from the main power grid, DG-1 must provide for all the power required for the local and common loads. We will consider both modes in the subsequent sections [24], [25]. A comprehensive review of dc microgrids can be found in [26]-[28].

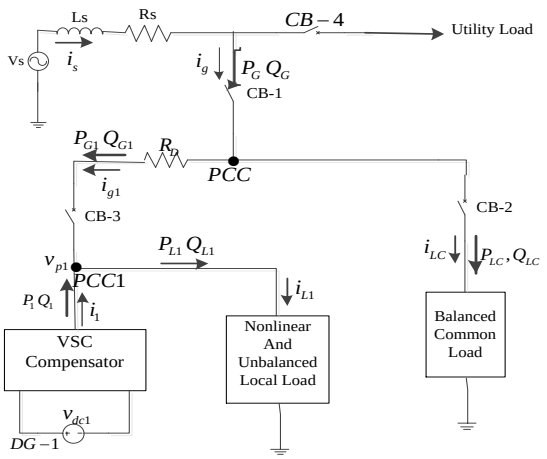

Fig. 1: Single-line diagram of the system including a microgrid, main power grid, and local and common loads.

As mentioned previously, the structure of the VSC is as shown in Fig. 2.

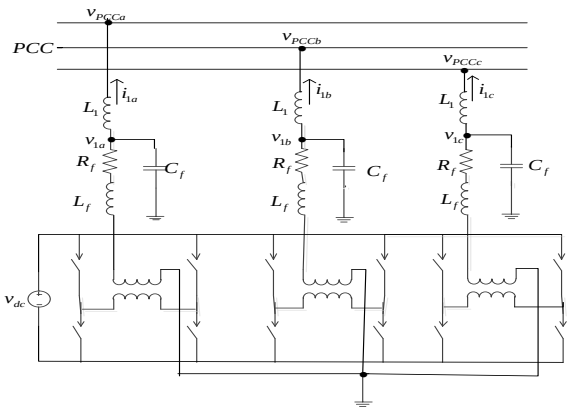

Fig. 2: VSC structure.

LQR Controller Design

The LQR controller is a type of state feedback controller, in which the control signal is determined in such a way that the cost function J is minimized.

$$J = \int_0^\infty x^T(t)Qx(t) + u_c^T Ru_c(t)d(t) \quad (1)$$

In (1), Q is a symmetric positive semi definite matrix, and R is a symmetric positive definite matrix.

As such, the control signal is obtained from the relationship uc=-kx. where k is obtained from the following relationship:

$$k = R^{-1}B^{T}S \tag{2}$$

In (2), S is obtained from the solution of the algebraic Riccati equations:

$$A^{T}S + SA + Q - SBR^{-1}B^{T}S \tag{3}$$

the matrices Q and R are the weighting matrices.

The matrix Q specifies the weights associated with the system states [4], [29] this means that states with higher importance have higher weights, and the values of their corresponding elements in the matrix Q are higher. The matrix R specifies the weights associated with the control signals.

The dimensions of the weighting matrices are determined according to the number of the states or control signals. In the current control method, the matrix Q is considered to be of dimensions 1×3, and the matrix R is considered one-dimensional, corresponding to the input control signal, given the derived state equations. The control signal is considered to be u_c and is specified in such a way as to minimize the cost function J. Here, the cost function has been defined in such a way that its goal is to minimize the control signal and the states. The larger the number used in the weighting matrix R, the smaller the control signal u_c will be, and the less costly the designed system will be. In the next section, we will introduce the proposed DEMPC along with the selected number of switching states.

Model Predictive Controller

The MPC method is an optimization problem in which the cost function is minimized. Using the system's model and the variable values up to the time K, the state values are predicted up to the time horizon K+N. In addition, the first component of the command sequence is applied at the time K+1 by optimizing the cost function. These steps are repeated for the subsequent time steps.

The cost function contains the control goals of the system, and its common terms include certain variables, which must follow a reference value [24]. According to (4), controlling these variables will in the form of a function of the error in the predicted value and its reference value.

As seen in (4), this function can be a magnitude, the square of a value, or an integral during a sampling period.

$$g = \int_{k}^{k+1}\left(x^{*}(t) - x^{p}(t)\right)dt \tag{4}$$

A. Finite Set Model Predictive Control

This method leverages the discrete nature of electric power converters, such that all the voltage vectors of the converter are tried in the cost function, and the vector that minimizes the cost function is selected [26], [30].

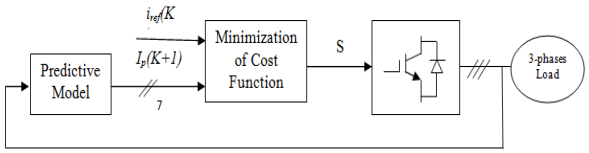

Fig. 3: FS-MPC diagram for the three-phase inverter.

Fig. 3 displays the FS-MPC diagram. The solution algorithm of this method consists of the following steps:

1. Load current measurement

2. Load current prediction in the subsequent sample for all possible switching states, according to the following relationship:

$$i_p(k+1) = (1 - \frac{r_L \times T_S}{L})i(k) + \frac{T_S}{L}(v_S(k) - v\{s_i\})) \tag{5}$$

Equation (5) has been obtained by discretizing the converter's voltage relationship.

3. Evaluation of the cost function for each prediction In this method, the cost function is expressed as the error between the reference current and predicted current for each possible switching state, according to (6).

$$g[n] = \left|i_{\alpha ref} - i_{\alpha p}\{S_i\}\right| + \left|i_{\beta ref} - i_{\beta p}\{S_i\}\right| \tag{6}$$

4. Selection of the switching state that minimizes the cost function. When FS-MPC designs are implemented experimentally, a large volume of computations is performed in the sampling period, which causes a considerable delay in the actuator signal. Hence, ignoring the delay due to measurement, computations, and actuator signal in the controller design will lead to the weak performance of the controller. The reason for this delay and the method of compensating it has been explained in [14].

Proposed DEMPC

The model used for prediction is a discrete-time model that can be expressed as state equations according to (7)-(8).

$$x(k+1) = Ax(k) + Bu(k) \tag{7}$$

$$y(k) = Cx(k) + Du(k) \tag{8}$$

In these equations, the vector x(k) represents the current values of the state variables, x(k+1) denotes the predicted values of the state variables, u(k) is the current values of the input variables, and y(k) is the vector of the current output values.

The cost function must be specified in the subsequent step. According to (9), in this function, the reference values, the future state variables, and the future control commands are considered.

$$J = f\big(x(k), u(k), \dots\dots\dots\dots, u(k+N)\big) \tag{9}$$

The DEMPC method is an optimization problem in which the cost function is minimized. In this optimization, the system's model and the control goals are considered for the time steps K+1 to K+N. The outcome of this optimization is N sequential commands, and the first component of the command sequence is applied at the instant K+1. Similarly, using new measurement values during this time, optimization is performed for the subsequent instant, and the appropriate command is selected for the instant K+2. This type of computation is known as the receding horizon strategy.

The functioning of DEMPC is shown in Fig. 6. Using the system model and the values of the variables up to the time K, the state values are predicted up to the time horizon K+N.

In addition, the first component of the command sequence is applied at the time K+1 by optimizing the cost function. These steps are repeated for the subsequent time steps.

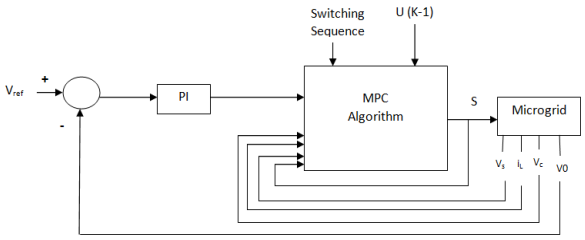

Fig. 4: Block diagram of the implemented control method

According to Fig. 4, a number of switching states for controlling the microgrid have been defined in this method, and the switching is performed according to these states and the cost function.

A. Proposed Method

The Single-phase equivalent circuit of converted is shown in Fig. 1.

Using this figure and in presence of the LCL filter, the state vector in conventional methods is considered as below:

$$x_1^T = \begin{bmatrix} i_f & i_1 & v_{cf} \end{bmatrix} \tag{10}$$

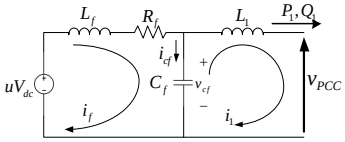

Fig. 5: Single-phase equivalent circuit VSC (LCL filter).

Fig. 5 shows the block diagram of the implemented control method. It is easy to produce reference values for the output voltage v_{cf} and the current i_c from the load distribution conditions; however, producing the reference value for the current i_f is difficult. For simplicity, we define the new state vectors as follows:

$$x^T = [i_c \quad i_1 \quad v_{cf}] \tag{11}$$

Thus, the following state transformation matrix will be obtained:

$$x = \begin{bmatrix} 1 & -1 & 0 \\ 0 & 1 & 0 \\ 0 & 0 & 1 \end{bmatrix} x_1 = C_p x_1 \tag{12}$$

The transformed state equations are obtained as follows by the combination of (11) and (12).

$$\dot{\mathrm{x}} = \mathrm{C_p A C_p^{-1} x} + \mathrm{C_p B u_c} + \mathrm{C_p C v_{pcc}} = \Lambda \mathrm{x} + \Gamma_1 \mathrm{u_c} + \Gamma_2 \mathrm{v_{PCC}} \tag{13}$$

The control law is defined as follows:

$$u_c(k) = -K\big[x_1(k) - x_{ref}(k)\big] \tag{14}$$

In the above relationship, K is a gain matrix, and x_{ref} denotes the reference vector. The gain matrix can be obtained using the DEMPC method and the proposed switching method. The control law in (14) includes switching control, which is discussed in details as follows:

Assuming full controllability on u, we can design a second-order steady-state linear optimal controller for this problem. As mentioned previously, the control law is as follows:

$$u = -K\big[x_1(k) - x_{ref}(k)\big]$$

In the above$x_{ref}(k)$, represents arbitrary state vectors. The DEMPC minimizes the following performance index:

$$j = \int_0^\infty \{(x - x_{ref})^T Q (x - x_{ref}) + \rho u^T R u\} dt \tag{15}$$

The index given in (15) must be minimized to obtain the optimal control law u by solving the steady-state Riccati equations. In (15), the weighting matrix Q is a positive definite or semi-definite, real, and symmetric matrix, and the penalty control matrix R is a positive definite, real, and symmetric matrix. Moreover, ρ is a

positive constant. Based on Brison's rule, the initial selections of the matrices R and Q are possible as diagonal matrices, as follows:

$$Q_{ii} = \frac{1}{maximum\ acceptable\ value\ for\ z_i^2} \quad i\epsilon\ \{1, 2,\ldots, l\}$$

$$R_{jj} = \frac{1}{maximum\ acceptable\ value\ for\ u_j^2} \quad j\epsilon\ \{1, 2,\ldots, m\} \quad (16)$$

In the above relationship, l is the number of control outputs, and m represents the number of inputs. z_i is called the controlled output and is related to the signal we would like to minimize to the lowest possible value in the shortest possible time.

In this method, the output voltage is adjusted indirectly by controlling the inductor current. To this end, an optimal objective function, which determines the switching order, is specified.

The switching order along the predictor's horizon is as in (17):

$$U(k) = [u(k)\, u(k+1) \ldots u(k+N-1)]^T \quad (17)$$

U is the optimal switching state, the first element of which u(k) is applied to the circuit, and the rest of its elements are applied at subsequent times.

In this method, one can consider one of the control goals of the objective function to be reducing the difference between the current and the reference value, according to (18).

$$\mathrm{i}_{Lerr}(\mathrm{k}) = \left|\mathrm{i}_{Lref}(\mathrm{k}) - \mathrm{i}_L(\mathrm{k+1})\right| \quad (18)$$

As such, the cost function can be expressed as in (19):

$$J(k) = \sum_{j=k}^{k+N-1} \cdot \left[i_{Lerr}(j \mid k)\right] \quad (19)$$

The optimal switching state is obtained by minimizing the cost function:

$$U^*(\mathrm{k}) = \arg\min \mathrm{J(k)} \quad (20)$$

Optimal switching (20) is performed using the iteration method.

All the possible switching states are defined for the controller along the horizon of predictor N, which is denoted U(k).

As such, there will be N2 switching states. For all the switching states, the matrices (17) and (18) are computed, and the cost function (19) is also calculated. Finally, a switching state with the minimum value of J is selected and applied to the switch.

The existing differential approximation, i.e., di/dt, can be considered as follows as a simple step-forward Euler equation:

$$\frac{di_{\alpha,\beta}}{dt} \approx \frac{\mathrm{i}_{\alpha,\beta}[\mathrm{k+1}] - \mathrm{i}_{\alpha,\beta}[\mathrm{k}]}{\mathrm{T_s}} \quad (21)$$

In addition, by substituting (19) into (20), the future value of the load current vector is obtained as follows:

$$i[k+1]_{\alpha,\beta} = \frac{T_s}{L}\left(v_{\alpha,\beta}[k] - i_{\alpha,\beta}[k]\left(R - \frac{L}{T_s}\right)\right) \quad (22)$$

This equation is used in the controller block to predict the future values of the current from the measured voltage vector.

In the predictive control method, the existing switching vectors on control system response are measured using error function definition, and an appropriate vector is selected based on a generated error in the cost function.

Here, measured inverter currents in space αβ are compared with reference values in this space, and the switching vector with the least error is selected. Hence, error cost equations will be driven using equation (23) of the paper.

To select the voltage vector for controlling the current, the predicted current is evaluated using the following cost function:

$$g[k+1] = |i_\alpha^*[k+1] - i_\alpha[k+1]| + \left|i_\beta^*[k+1] - i_\beta[k+1]\right| \quad (23)$$

where i*α,β[k+1] is an estimate of the reference current vector in the subsequent horizon. For grids with sufficiently small sampling time, one can assume that this current is equal to its previous values, i.e.: i*α,β[k+1] ≈ i*α,β[k].

However, for large sampling times, the future value of the reference function must be extrapolated.

The cost function in the proposed algorithm is the minimization of the voltage drop. The objective function that must be minimized is defined as follows:

$$F = \int_0^{t_{sim}} t.\sum(|P_i - P_{iss}| + |Q_i - Q_{iss}|)dt, i = L_1, G_1, 1, L_2, G_2, 2 \quad (24)$$

In the above equation, PG1ss, PL1ss, PL2ss, P2ss, and PG2ss are the final (steady-state) values obtained for the real powers in Table 1. In addition, Q1ss, QL1ss, QG1ss, Q2ss, QL2ss, and QG2ss are the final (steady-state) values of the reactive powers.

This objective function has been defined in such a way that the power values have the smallest deviation from the final or steady-state values and reach their steady states in the shortest possible time.

Also, we should note about equation (23) in this paper that the performance of predictive controller cause creating balance in voltage and current, and system power quality will be desired to a good degree, but during separating microgrid from the primary grid

(island mode occurrence) and changing this mode, it has seen that we need a period to system reach balance state.

The MPC algorithm for controlling the current in the mentioned system is as follows:

- Application of v[k]
- V[k-1]=v[k]
- Measurement of the currents ia, ib, and ic
- calculation of the current vector
- Prediction of the subsequent horizon's current i[k+1]
- Calculation of the cost function g_i
- If $g_i<g_{opt}$
  - Yes: $g_{opt}=g_j$, $I_{opt}=I_j$
  - No: Restart

Simulation Results

As mentioned in Fig. 1, the system considered in this section contains a DG source. The microgrid is connected to the main grid at the point PCC. The DG source has local loads, including unbalanced and nonlinear loads.

In the grid-connected mode, the common load is fully supplied by the grid, and the power required for the local load is jointly supplied by the source DG-1 and the grid.

In the islanding mode, i.e., when CB-1 is opened and the microgrid is disconnected from the main power grid, DG-1 must provide for all the power required for the local and common loads.

We will consider both modes in the subsequent sections.

A. Local Load Supply Jointly with the Main Power Grid (Grid-Connected Mode)

In this section, the supply of the local DG load by sharing this load between the main power grid and the DG source will be presented.

Since the DG source does not supply the common load, the following holds:

$\lambda_{1PG} = \lambda_{1QG} = 1.$

Let us assume that, in this case, we would like the system to behave in such a way that DG-1 provides for 10% of the real power and 20% of the reactive power of its local load according to plans. Therefore, in this case, the following is true:

$\lambda_{1P} = 0.1, \lambda_{1Q} = 0.2.$

The system data, including the characteristics of the load, VSC, and voltage sources, are shown in Table 1.

Let us assume that at t=0.5s, the impedance of the common load is reduced to half the initial value. Fig. 5 displays the sharing of the real and reactive powers for the source DG-1.

The voltage of point (PCC1) and the current ig1 are shown in Fig. 6.

The load allocation with the desired ratios and the voltage balance even after a change in the common load indicate the stable performance of the microgrid.

It must be noted that for balance in the grid and optimal load allocation, the state feedback control law mentioned in Section 3 has been used.

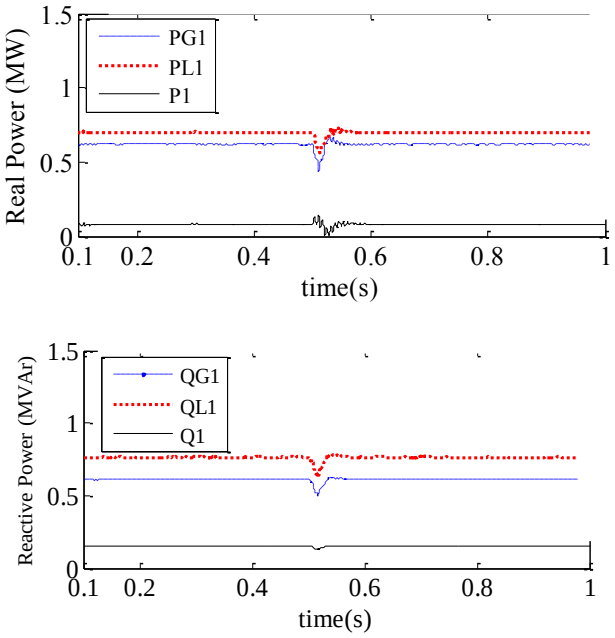

Fig. 6: Allocation of real and reactive powers in the grid-connected mode (for a system including one DG): (a) real power (MW); (b) reactive power (MVar).

In this example, for the adequate performance of the grid, the characteristic parameters of LQR are selected as follows:

$Q = diag[0\ 1\ 1] \quad R = 0.05, \rho = 1$

K= [8.1109 3.2170 0.1170] where diag is a diagonal matrix. The two most important variables for control are the current i_l and the voltage v_{cf}. The choice of the matrix Q indicates the significance of these states.

In Figs. 6 and Fig. 7, voltage droop and, hence, a drop in the real and reactive powers at the instant of change in the load (i.e., 0.5s,) are clearly observed.

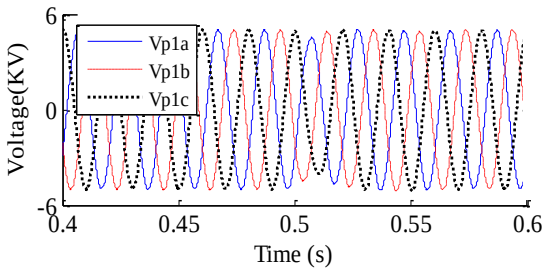

Fig. 7: (a) Three-phase voltage at the point PCC1.

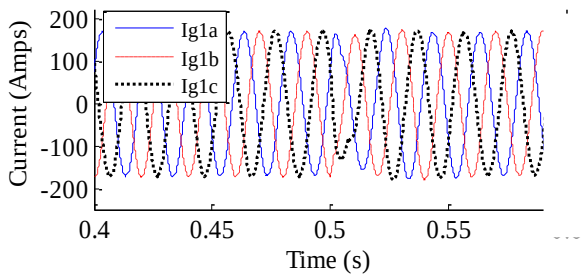

Fig. 7: (b) Current injected by the grid at the point PCC1.

Table 1: Parameters of the system in Fig. 1

System quantities	Values
System frequency	50 HZ
Voltage source (Vs)	"11 KV rms"("L-L")
Feeder impedance	Rs=1.025Ω, Ls=57.75 mH
Unbalanced local load	$R_{La} = 48.4\Omega, L_{Lb} = 192.6mH$ $R_{Lb} = 24.4\Omega, L_{Lb} = 100.0mH$ $R_{Lc} = 96.4\Omega, L_{Lc} = 300.0mH$
Nonlinear local load	A three-phase rectifier including a resistive-inductive load with values of R=200Ω and L=200mH

After a short amount of time (about 0.025s), the voltage, current, and powers return to the balanced state. Some of the numerical results of these graphs are shown in Table 2.

Table 2: Numerical results of the grid-connected mode

Real/reactive Power Fig. 5	Initial Value (MW)	Final Value (MW)	Minimum Value (t=0.5)	Maximum undershoot (MV)
PL1	0.7	0.7	0.56	0.14
PG1	0.628	0.63	0.44	0.17
P1	0.072	0.07	0.003	0.067
QL1	0.76	0.76	0.62	0.14
QG1	0.61	0.61	0.5	0.11
QL1	0.15	0.15	0.12	0.03
Fig. 6 Voltage Droop	Voltage Range		Current Range (AMP)	
4.5%	5		175	

B. Investigation of the Islanding Mode

Let us consider the system mentioned in the previous section.

Also, let us assume that at time t=0.4s, CB-1 opens, and islanding occurs while the common load is still connected to the system. In this mode, both the common load and the local load must be fully supplied by the DG unit.

Also, in this mode, the values of λ are considered as follows:

$$\lambda_{1PG} = \lambda_{1QG} = 0 \text{ And } \lambda_{1P} = \lambda_{1Q} = 1$$

Moreover, the LQR characteristic parameters are selected as before.

Fig. 8 shows the distribution of real powers, and Fig. 9 displays the voltage at the point PCC1. As soon as islanding occurs, the voltage droop at the point PCC1 leads to a slight drop in the power required for the local load PL1.

Meanwhile, the power generated by DG-1, namely P1, increases to supply the power required for the common load shown in the figure by the negative value of PG1.

The negative value for the power PG1 in Fig. 8 indicates the power flow in a direction opposite to that shown in Fig. 1.

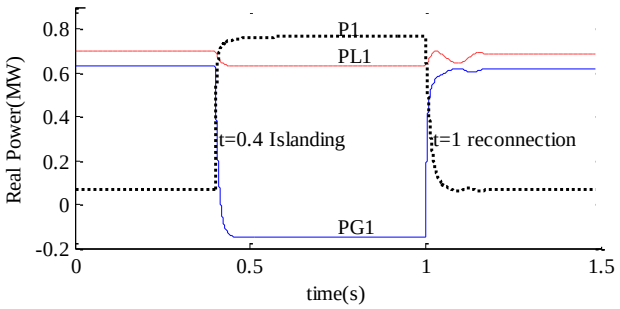

Fig. 8: Allocation of real powers in DG-1 in the islanding mode.

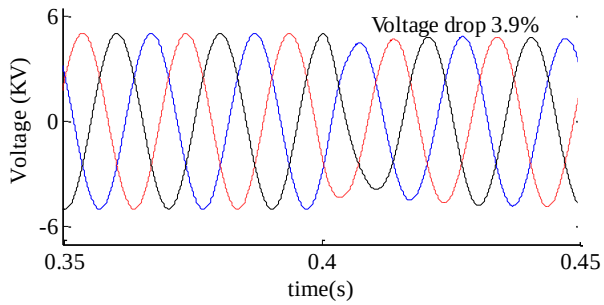

Fig. 9: Three-phase voltage at the point PCC1.

At time t=1s, CB-1 is again closed, and the system returns to the grid-connected mode. As seen in Fig. 8, after the reconnection of the circuit breaker at t=1s, the

system is not balanced immediately, and some time (about 0.17s) is required for the powers to reach their initial values. In addition, the values of the real powers at these instants have slight overshoot and undershoot relative to their balanced states. Some of the characteristics of these graphs are shown in Table 3.

Table 3: Numerical results of the islanding mode

Real power Fig. 5	Initial value (MW)	intermediate in the Islanding mode	Final value (MW)	Recovery time (s)
P_{L1}	0.7	0.63	0.6	0.17
PG1	0.629	-0.13	0.625	0.16
P1	0.071	0.76	0.07	0.17
Fig. 8	Voltage Droop	initial value	Intermediate value in the islanding mode	
PL1	3.9% OV% 3%	5 rise time 0.08s	4.8 ettling time 0.25s	

Let us consider the microgrid mentioned in Fig. 1. There, we observed that the transient response of the system was not adequate upon the occurrence of the islanding mode and the reconnection to the grid, and the return of the power distribution to the stable state took some time.

To resolve this issue, the simulation results of the DEMPC method have been obtained.

C. Performance of the Proposed Controller

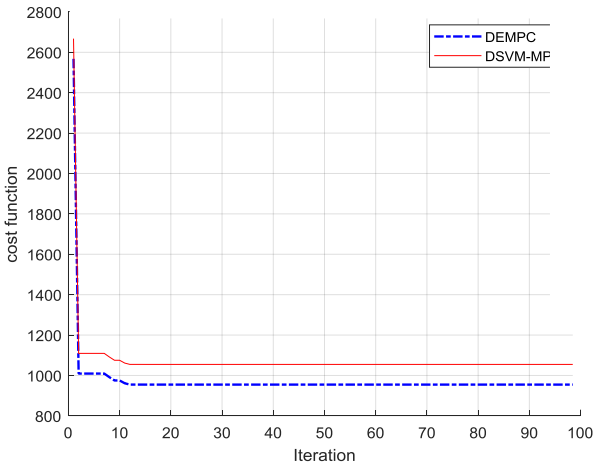

Fig. 10: Convergence graph of the DEMPC algorithm comparison to LQR.

Fig. 10 displays the convergence graph of the objective function.

Studying the convergence graph in the MPC method and LQR method helps us evaluate the performance of the cost function of the microgrid.

Fig. 11 shows the allocation of real powers, and Fig. 12 displays the voltage at the point PCC1 in the presence of DEMPC. The numerical results of these graphs are shown in Table 4.

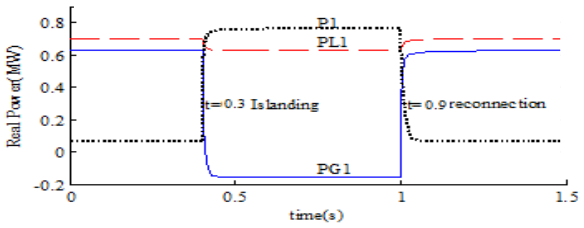

Fig. 11: Distribution of DG-1 real powers in the presence of DEMPC.

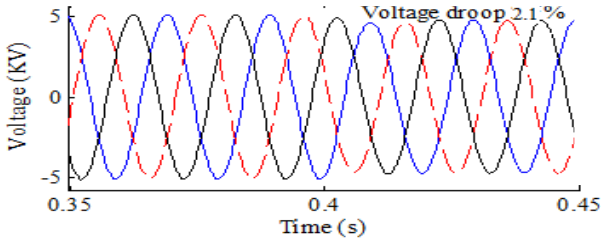

Fig. 12: Three-phase voltage at the point PCC1 in the presence of DEMPC.

According to Fig. 12 and the data shown in Table 3, in the presence of DEMPC, the transient response of the system has improved to a suitable level, and, after the reconnection of the grid, the power distribution recovers at a shorter time compared to the LQR controller. The results are given that in Table 4, to evaluate the performance of the proposed controller with FS-MPC and DSVM-MPC methods in this regard. As can be seen, proposed controller shows better performance in islanding mode compared to other ones.

As shown in Table 4, at t=1s, CB-1 closes again, and the system acts with the model predictive controller this time and returns to the grid-connected mode. As seen in Fig. 10, after the reconnection of the circuit breaker at t=1s, the system immediately regains balance, and only about 0.02s is required for the powers to reach their initial values.

In addition, the values of the real powers that had slight overshoot and undershoot at these instants are now in their balanced states with the DEMPC method.

Table 4: The numerical results for the islanding mode in the presence of DE-MPC and comparison to FS-MPC and DSVM-MPC

Real power Fig. 10	Initial value (MW)	intermediate in the Islanding mode	Final value (MW)	Recovery time (s)
P_{L1}	0.7	0.68	0.7	0.02
PG1	0.63	-0.12	0.63	0.02
P1	0.071	0.71	0.07	0.03

Fig. 11	Voltage Droop	initial value	Intermediate value in the islanding mode
DEMPC	2.1%	5	4.89
FS-MPC	2.7%	5	4.85
DSVM-MPC	2.5%	5	4.87
PID	2.5%	5	4.89

PL1	OV%	rise time	settling time
	0	0.05s	0.1s

Moreover, in Table 4 Obtained simulation results are mentioned in Table 4 to compare the proposed method with PID controller using (PSO algorithm), FS-MPC and DVSM-MPC methods. As a consequence proposed method is much more effective than conventional control methods. Additionally, in the recovery state of the grid, real power values experience a little overshoot and undershoot. With the appropriate selection of index parameters of the predictive controller LQR and other methods, we could improve the transient performance of the system. To do that, will well discuss calculating index parameters if controllers for microgrid include a distributed generation source using evolutionary particles swarm algorithm, which is shown in Fig. 9.

Conclusion

In this research, a model predictive controller was proposed. A comparison of these waveforms with the results obtained in Tables 3 and 4 revealed that the proposed distributed economic model predictive controller significantly improves the transient response of the system and the power quality of the grid compared to the LQR, PID, FS-MPC and DVSM-MPC methods. It must be mentioned that the proposed distributed economic model predictive controller has performed more successfully in creating balance and stability in the microgrid in the grid-connected mode. In addition, this paper proposes a novel PCC voltage compensation method for islanded microgrids by improving the power sharing control schemes among the DGs to compensate for the PCC voltage deviation caused by the droop control and the state feedback controller.

As a result, the recovery time for re-switching from the island mode to the connection mode of the distributed generation sources is reduced. Hence, the following state transform matrix is considered for this system, and better results in terms of overshoot, rise time, settling time, and steady-state have been obtained with this method.

Author Contributions

I. Sayedi designed the simulation, collected data, experiments and interpreted the results. M.H. Fatehi wrote the manuscript. M. simab carried out the data analysis.

Acknowledgment

The authors received no funding from any organization in the course of carrying out the current study. It is certified that the Islamic Azad University is a private research and academic institute.

Conflict of Interest

The author declares that there is no conflict of interests regarding the publication of this manuscript. In addition, the ethical issues, including plagiarism, informed consent, misconduct, data fabrication and/or falsification, double publication and/or submission, and redundancies have been completely observed by the authors.

Abbreviations

DEMPC	Distributed economic Model Predictive Control
VSC_s	Voltage Source Converters
DG	Distributed Generation
LQR	Linear Quadratic Regulator
UPS	Uninterruptible Power Supply
VSI_s	voltage source inverters
FS-MPC	Finite Set Model Predictive Control
DVSM-MPC	Discrete Space Vector Modulation

References

[1] K. Rajesh, S. Dash, R. Rajagopa, R. Sridhar, "A review on control of ac microgrid," Renewable Sustainable Energy Rev., 71: 814-819, 2019.

[2] M. Liangyu, Y. Kwang, G. Yinping , "An improved predictive optimal controller with elastic search space for steam temperature control of large-scale supercritical power unit," in Proc. 51st IEEE Conference on Decision and Control (CDC), 2012 .

[3] W. Tong, G. Huijun, Q. Jianbin, "A combined adaptive neural network and nonlinear model predictive control for multirate networked industrial process control," IEEE Trans. Neural Networks Learn. Syst., 27(2): 416-425, 2015.

[4] P. Buduma, G. Panda, "LQR based control method for grid connected and islanded DG system," Int. J. Emerging Electr. Power Syst., 19(5), 2018.

[5] M. Alhasheem, F. Blaabjerg, P. Davari, "Performance assessment of grid forming converters using different finite control set model predictive control (FCS-MPC) algorithms," Appl. Sci., 9(17): 1-14, 2019.

[6] W.R. Sultana, S.K. Sahoo, S. Sukchai, S. Yamuna, D.A .Venkatesh, "Review on state of art development of model predictive control for renewable energy applications," Renew Sustain Energy Rev., 76: 391-406, 2017.

[7] C. Jiang, G. Du, F. Du, Lei Y, "A fast model predictive control with fixed switching frequency based on virtual space vector for three-phase inverters," in Proc of the IEEE International Power Electronics and Application Conference and Exposition, PEAC, Shenzhen, China, 2018.

[8] M. Aguirre, S. Kouro, C.A. Rojas, J. Rodriguez, J. Leon, "Switching frequency regulation for FCS-MPCBased on a period control approach," IEEE Trans. Ind. Electron, 65(7): 5764-5773, 2018.

[9] H. Yang, R. Tu, K. Wang, J. Lei, W. Wang, S. Feng, C.A. Wei, "Hybrid predictive control for a current source converter in an aircraft DC microgrid," Energies, 12(21): 4025, 2019.

[10] T. Qingfang, X. Ruiqi, "Integral sliding mode-based model predictive current control with low computational amount for three-level neutral-point-clamped inverter-Fed PMSM drives," IEEE Trans. Energy Convers., 35: 2249–2260, 2020.

[11] W. Wang, C. Liu, S. Liu, H. Zhao, "Model predictive torque control for dual three-phase PMSMs with simplified deadbeat solution and discrete space-vector modulation," IEEE Trans. Energy Convers., 36(2): 1491–1499, 2021.

[12] T. Dragi˘cevi´c, X. Lu, J.C. Vasquez, "DC microgrids-part II: A review of power architectures, applications, and standardization issues," IEEE Trans. Power Electron., 31: 3528–3549, 2016.

[13] T. Dragi˘cevi´c, X. Lu, J.C. Vasquez, J.M. Guerrero, "DC microgrids-part I: A review of control strategies and stabilization techniques," IEEE Trans. Power Electron., 31: 4876–4891, 2016.

[14] T. Dragi˘cevi´c, X. Lu, J.C. Vasquez, "DC microgrids-part II: a review of power architectures, applications, and standardization issues," IEEE Trans. Power Electron., 31: 3528–3549, 2016.

[15] N. Melanie, C. Jones, M. Morari, "Real-time suboptimal model predictive control using a combination of explicit MPC and online optimization," IEEE Control Syst. Soc., 56(7): 1524-1534, 2011.

[16] M. Khooban, N. vafaman, T. Niknam, T. Dragicevic, F. Blaabjerg, "Model-predictive control based on Takagi-Sugeno fuzzy model for electrical vehicles delayed model," IET Electr. Power Appl., 11(5): 918–934, 2017.

[17] M. Gillespie, C. Best, E. Townsend, et al., "Learning nonlinear dynamic models of soft robots for model predictive control with neural networks," in Proc. IEEE International Conference on Soft Robotics (RoboSoft), 2018.

[18] G. Romos, E. Lucas, C. Fernández, "Model predictive control performance optimized by genetic algorithm," Model Predictive Control, Springer, 93-108, 2019.

[19] G. Pathak, B. Singh, B. Panigrahi, "Three-phase four-wire wind-diesel based microgrid," Power Systems (ICPS), in Proc. IEEE 6th International Conference on Power Systems (ICPS), 2016.

[20] X. Luo, J. Wang, M. Dooner, j. Clarke, "Overview of current development in electrical energy storage technologies and the application potential in power system operation," Appl. Energy, 137: 511-536, 2015.

[21] U. Krishnan, S. Mija, E. Cheriyan, "State space modelling, analysis and optimization of microgrid droop controller," in Proc. 6th International Conference on Computer Applications In Electrical Engineering-Recent Advances (CERA), 2017.

[22] J. Lee, H. Moon, K. Lee, "An improved finite set model predictive control based on discrete space vector modulation methods for grid-connected three-level voltage source inverter," IEEE J. Emerging Sel. Top. Power Electron., 6(4): 1744–1760, 2018.

[23] J. Rohten, J. Muñoz, E. Pulido, J. Silva, "Very low sampling frequency model predictive control for power converters in the mediumand high-power range applications," Energies, 14(1): 199, 2021.

[24] M. Ghanbarian, M. Nayeripour, A. Rajaei, F. Jamshidi, "Model predictive control of distributed generation micro-grids in island and grid connected operation under balanced and unbalanced conditions," J. Renewable Sustainable Energy, 9(4), 2017.

[25] T. Morstyn, B. Hredzak, V. Agelidis, "Cooperative multi-agent control of heterogeneous storage devices distributed in a dcmicrogrid," IEEE Trans. Power Syst., 31: 2974–2986, 2016.

[26] Y. Shan, H. Jiefeng, L. Zilin, M. Josep, "A model predictive control for renewable energy based AC microgrids without any PID regulators," IEEE Trans. Power Electron., 33(11): 9122–9126, 2018.

[27] Y. Wang, X. Wang, Y. Xie, F. Wang, "deadbeat model predictive torque control with discrete space vector modulation for PMSM drivers," IEEE Trans. Ind. Electron., 64(5): 3537–3547, 2017.

[28] T. Elsayed, A. Mohamed, O. Mohamed, "DC microgrids and distribution systems: An overview," Electric. Power Syst. Res., 119: 407–417, 2014.

[29] R.N. Beres, X. Wang, M. Liserre, F. Blaabjerg, C.L. Bak, "A review of passive power filters for three-phase grid-connected voltage-source converters," IEEE J. Emerg. Sel. Top. Power Electron., 4: 54–69, 2016.

[30] F. Donoso, R. C´ardenas, H. S´aez, "finite-set model-predictive control strategies for a 3L-NPC inverter operating with fixed switching frequency," EEE Trans. Ind. Electron., 65 (5): 3954-3965, 2018.

Biographies

Iman Sayedi received his B.S. degree in Electrical Engineering from Sajjad University, Mashhad, Iran in 2007. He graduated in M.Sc. degree in Electrical Engineering and control system from Shahid Bahonar University of Kerman, Iran in 2010. Currently he is a Ph.D. student in Islamic Azad University Marvdasht branch, Iran. His interests include power system control, stability and evolutionary computation, MPC control systems in distributed generator (DG) in large control systems.

Mohammad H. Fatehi was born in Shiraz, Iran, 1982 and received the B.S. degree from Department of Electrical Engineering, Najafabad branch, Islamic Azad University in 2005 and M.Sc. degree in Control Engineering from Department of Electrical/Control Engineering, MUT University of Tehran, Iran in 2009. Also he received Ph.D. degree from Department of Electrical/Control Engineering, Islamic Azad University, Tehran in 2015. Dr. Mohammad H. Fatehi is currently Assistant Professor at Department of Electrical and Computer Engineering, Kazerun branch, Islamic Azad University, Iran. His current research is about bio-engineering, power-engineering, also modeling and control of Robotic systems.

Mohsen Simab (S'08, M'12) was born in Iran, on June 30, 1981. received the BSc degree in Electrical Engineering from Amir Kabir University, Tehran, Iran, and the MSc and Ph.D. degrees from Tarbiat Modares University, Tehran, Iran, in 2003, 2005, and 2011, respectively. He is an Assistant Professor in power systems at the Department of Electrical Engineering, Marvdasht Branch, Islamic Azad University, Marvdasht, Iran. His main research interests are electric distribution regulation, power system operation, and power system reliability.

How to cite this paper:
I. Sayedi, M.H. Fatehi, M. Simab, "The effects of the model predictive controller compared to the LQR controller on the optimal distribution of the suitable load and the creation of balance in microgrids," J. Electr. Comput. Eng. Innovations, 10(1): 231-242, 2022.

DOI: 10.22061/JECEI.2021.8194.489

URL: https://jecei.sru.ac.ir/article_1611.html